PREDICTION OF CRACKING UNDER THERMAL FATIGUE

A. Fissolo [1], C. Robertson [2], V. Maillot [3], B. Marini [1]

[1] CEA-CEREM
Commissariat à l'Energie Atomique – Saclay, 91191 Gif sur Yvette Cédex, France
[2] FX conseil – Ecole Polytechnique, Palaiseau, France
[3] Ecole Centrale de Lille
Cité Scientifique – BP48, F59651 Villeneuve d'Ascq, France

ABSTRACT

Thermal fatigue behaviour of 316L steel has been investigated. Two distinct tasks are presented here. The first one concerns the experimental determination of crack initiation conditions and early damage accumulation mechanisms. The second one is devoted to crack growth dynamics. The proposed models focused on the experimentally observed case of multiple cracking, under thermal fatigue loading conditions. In spite of simplified assumptions, the model predictions are in good agreement with observations, concerning both the mean and maximum crack in function of the number of cycles, up to N = 35000.

INTRODUCTION

Various components, find in different types of nuclear reactors are submitted to thermo-mechanical loading effects. In LMFRs for example, strong thermal fluctuations generated by the mixing of two flows of sodium at different temperatures or by a cyclic movement of sodium stratification interface constitute possible causes for the growth of crack networks [1]. Thermal fatigue cracking has been observed in PWR components as well, in spite of relatively small temperature fluctuations observed in RIS or RRA loops of the primary cooling circuit [2]. In future fusion reactors, first wall and blanket structural materials would be submitted to thermo-mechanical loading due to both a cyclic mode of operation and a high probability of dynamic loading by plasma disruption.

Thermal fatigue damage has been investigated in 316L steel, which is a reference material for nuclear reactor structures. A first task deals with crack initiation phase, which may correspond to a very important part of the total component life. A second action is devoted to the crack growth, in the case of single crack and multiple cracking conditions.

EXPERIMENTAL

Material

The tested material is an AISI 316L stainless steel with chemical composition as reported in Table 1.

TABLE 1

CHEMICAL COMPOSITION (WT %) OF 316 L STEEL

C	Ni	Cr	Mn	Cu	Mo	Si	Co	S	P	N	B	Fe
0.024	12.33	17.44	1.82	0.2	2.3	0.46	0.17	0.001	0.003	0.06	0.0008	Bal.

Thermal fatigue Facilities

In the present study, the investigation of thermal fatigue behaviour of 316L steel is performed by means of two complementary, distinct tests, which we will refer to as SLPASH and CYTHIA tests. The so-called SPLASH test is used to determine crack initiation conditions and to reproduce multiple cracking networks as observed in actual components, when submitted to in-service conditions. The CYTHIA test was originately designed to assess crack propagation dynamics for one isolated crack. It can also be used to investigate surface damage accumulation, as surface oxidation is far less severe than for SPLASH test.

SPLASH test is presented in Figure-1. The tested specimen is continuously heated by the passage of an electrical DC current. The hot specimen is then submitted to cyclic thermal downshock (about 1000°C/s) by means of periodical spraying of water on two opposite faces. In most tests, the selected surface temperature variation ranged from 300°C to 550°C, as indicated in Figure 2. The number of cycles to crack initiation N_i is deduced from regular examinations of the quenched (sprayed) surfaces, by means of optical microscopy. The initial roughness of these surfaces is accurately controlled ($Ra < 0.8$ μm). It is considered that initiation occurs when at least one 50μm to 150μm long crack is observed. Additional SPLASH tests were performed for $N >> N_i$, with a view to investigate the evolution of a surface multiple cracking network with the number of cycles N. After these tests, the 3D character of the final crack network is also examined, by means of a step by step removal of thin surface layers. Crack network morphological characteristics are recorded at each step, using an image analysis device.

The CYTHIA test is presented in Figure-3. Specimen consist of thick hollow tubes. During test, the tube external wall is periodically heated by means of a HF induction coil (1 MHz), while its internal wall is permanently cooled by flowing water. To insure single crack propagation, a sharp circumferential groove is spark-machined in the heated portion of the specimen (at the coil position). In most cases, crack growth dynamics is estimated after test, by examining the fracture surface of broken specimen. Post-test breaking is performed under mechanical fatigue loading conditions. Note that a strong oxidation treatment of the specimen surface is done before final breaking, in order to clearly distinguish between the thermal fatigue crack propagation zone and the final rupture zone. In some cases, in-test control of crack growth is performed as well, in order to make sure that test proceeds normally.

A similar temperature monitoring procedure is enforced in both SPLASH and CYTHIA tests. In both cases indeed, a few calibration tests are performed before each testing campaign, by means of one calibration specimen of each type. Calibration specimen possesses the same geometry as that of test

specimen, plus as many as 15 thermocouples[1]. These thermocouples, including one embedded on the heated/quenched surface, are positioned at regular spacing along wall thickness direction. In this way, experimental parameters, such as the quantity of sprayed water (SPLASH) or HF intensity (CYTHIA) are tuned, so as to obtained one specific specimen thermal mapping during test. Calibration specimen is then removed and test specimen is installed for a whole testing campaign. In order to make sure that experimental conditions do not change throughout test (which may last a few weeks or months), one control thermocouple is installed on each tested specimen.

Results

Crack initiation phase

In the present study, crack initiation refers to the detection of the first 50-150µm long cracks. In facts, smaller crack-like surface displacements may be initiated much earlier, due to localised surface damage accumulation or to any microscopic discontinuity. It can thus be proposed that, in most cases, the first initiated cracks (in the same sense as above) may correspond to early crack-like surface displacements that have propagated to some extent. In order to better understand thermal fatigue damage accumulation, thin foils extracted from the outer surface of CYTHIA specimen[2] have been observed in TEM. The dislocations arrangements showed in Figure-4 were produced after very small number of cycles (N = 100). These well defined slip bands are typical of fatigued 316L steel and indicate that strain localisation takes place at early stages of specimen fatigue life. In the present case, it is worth noting that these bands are present within surface-lying grains only (< 50µm), i.e. in foils extracted by means of the so-called back-side electropolishing technique. So as to how these microstructure may initiate cracking in the specimen surface is nevertheless far beyond the scope of the present paper.

Figure 5 shows the evolution of the number of cycles to cracking initiation N_i, as a function of the temperature range. Open symbols distinguish tests made with significant holding time. The cycling quenching frequency ranges between 0.025 and 0.25 Hz. It is observed that the selected temperature range significantly affects N_i. A very strong decrease of N_i is indeed observed when temperature range increases from 100°C to 300°C. When the temperature range is set at 300°C with a maximum temperature of 550°C, initiation appears after only 6000 cycles, whereas no initiation is detected, even after 1 000 000 cycles, when the temperature range is set at 125 °C (with the same maximal temperature). As in the case of isothermal mechanical fatigue thus, a thermo-mechanical endurance limit threshold is evidenced.

Multiple Cracking

All the results presented here were performed for one maximum temperature of 550 °C and surface temperature variations between 200°C and 250°C. After 300 000 cycles, cracking network development is very scarce when ΔT is 215°C, whereas cracking becomes well marked when ΔT is 230 °C. A very sharp transition may thus exist in that temperature range domain, for a low initial surface roughness and residual stresses.

Figure 6 underlines the importance of selected temperature variation during cycling, since a very dense crack network is observed after only 20 000 cycles, when ΔT is set to 250°C. A very strong decrease of the cracking density is observed at increasing depth, which means that while many cracks are progressively stopped, others continue to develop. No crack deeper than 700 µm has been detected after 20 000 cycles, and deeper than 2100 µm after 100 000 cycles. As it was suggested on Figure 7, crack network evolution

[1] One should note that calibration specimen are not suited for long testing campaigns, as thermocouple installation requires machining that can induce premature damage.

[2] Away from the spark-machined groove.

for N>20 000 cycles roughly corresponds to the extension of a few longer cracks. In any cases, crack spacing is about 150-200 μm at the surface, which corresponds to 1–2 grain size.

PREDICTION OF CRACK GROWTH UNDER A THERMAL FATIGUE LOADING: EARLIER MODELS AND IMPROVEMENTS

The proposed proposed models are based on experimental data in austenitic 316 L steel. These models do not account for any effect coming from additional stresses or roughness.

Prediction of initiation

If initiation is defined as before, i.e. it corresponds to the detection of the first 50-150 μm cracks, the French fast breeder code RCC-MR gives good prediction for N_i [3]. If temperature range is converted into a strain range, an equivalent strain–controlled isothermal fatigue curves can be computed from thermo-mechanical data. Figure-8 confirms the pertinence of comparing isothermal fatigue curves to thermo-mechanical equivalent curves. Nevertheless, tests performed with a holding time exhibited a significantly different behaviour. Thus, additional microstructural observations and simulations may prove necessary, particularly in case of more complex loadings and initial surface conditions.

Prediction of growth

Case of a single crack (geometrical or stresses singularities)

Prediction of single crack growth is a necessary step to determine more complex cases such as the extension of cracks embedded in multiple crack network. A cyclic strain intensity range $\Delta K\varepsilon$ may be defined as $\Delta\varepsilon\sqrt{\pi a}$ where $\Delta\varepsilon$ is a representative strain range. For uniaxial strain, the damaging strain can be expressed more accurately as $\Delta\varepsilon_p+q\Delta\varepsilon_e$ where $\Delta\varepsilon_e$ is the elastic strain range and $0.5 <q<1$ [4]. $\Delta\sigma_{equiv}$ is obtained upon multiplied by E, giving rise to an equivalent stress intensity parameter which has been proposed as a correlating parameter between High strain Fatigue and LEFM data [5 to 7]. Crack growth rate is deduced using a Paris relation. Note that this approach give results that are very similar to those obtained from a ΔJ energetic approach [8].

In our particular case corresponding to a cylindrical geometry (CYTHIA), the equivalent stress as a function of the depth is given by the following relation:

$$\Delta\sigma_{eq}(x) = q\Delta\sigma_{zz}(x) + \frac{E}{(1+\nu)(1-2\nu)}.[(1-\nu)\Delta\sigma_{zz} + \nu\Delta\sigma_{rr} + \nu\Delta\sigma_{\theta\theta}]$$

in the plastic domain, with $\sigma_{eq}=\sigma_{zz}(x)$ when plasticity becomes negligible, e.g. $\varepsilon_p \leq 10^{-4}$

The equivalent stress intensity factor is determined using the superimposition method [9]. If stress is fitted with a third degree polynomial, it can be expressed as:

$$\Delta K_{eq} = 1.12(\pi.a)0.5\left(A_0F_1 + \frac{2a}{\pi}F_2 + \frac{a^2}{2}A_2F_3 + \frac{4}{3\pi}a^3A_3F_4 \right) \text{ and } \frac{da}{dN} = C\Delta K_{eq}{}^m$$

where F_1, F_2, F_3, F_4 are calculated for the CYTHIA axisymetrical geometry, in the case of a uniform or variable ($p = x^i$ with $1 \leq i \leq 3$) pressure applied on the crack walls. This calculation is performed by the finite elements method, using CASTEM 2000 CEA software.

Comparison between measurements and calculated predictions is presented in Figure 9. Curves are determined for the average crack growth rate [10]. A value of q ranging between 0.6 and 0.8 generally gives good predictions [11]. With the maximum crack growth rate however, q would be rather close to 0.8.

Case of a multiple crack damage (straight parts)

Our goal is to estimate crack growth evolutions in the depth direction, which results in a reduction of the specimen resistant section. As showed by experiments, two separate steps must be distinguished for the multiple crack evolution: initiation and crack growth.
To simulate the initiation phase, surface grains are first generated using a Monte-Carlo randomisation method: grain size distributions are fitted to experimental observations. It is then assumed that each grain is cracked, an assumption that is also based on above discussed experimental results (i.e. a mean crack-crack distance of 150-200µm at the surface). It can be showed that the final results do not strongly depend on the initial number of cracked surface grains.

The evolution of a given crack included within a crack network is determined, using a similar but more general approach than that used in the case of single, isolated cracks. This generalisation accounts for mutual strain shielding effect arising between cracks, an effect that evolves continuously with crack growth. In the present model, cracks are taken as parallel infinite bands. In an earlier version of this model [12], the strain shielding effect felt by one particular crack was taken as the effect of the strongest interacting crack only. The later was determined by first computing the stress intensity factor (SIF) for each pairs of cracks, successively. The strongest interacting crack then obviously corresponds to that giving the smallest SIF value. F_1, F_2, F_3, F_4 factors may be then directly extracted from a pre-calculated table, as a function of pair depth and separation (a, b, d). The use of “pre-calculated evaluations” is much faster in terms of CPU time than the re-actualisation of mutual stresses during growth, using finite element method computations. The results presented in figure-10 show that simulated mean depth is close to experimental results, while the maximum depth is overestimated. Nevertheless, this method gives more realistic results that those derived from single crack growth prediction i.e. without considering any mutual interaction.

Mutual interactions during crack growth can be computed more accurately using step by step finite element calculations, with auto-adaptative meshing of the propagating cracked zones. Figure-11 shows calculations up to 35 000 cycles for as many as 10 cracks, when the complete crack-crack interactions are accounted for. The number of finite elements is keep as low as possible, using refined meshing in the vicinity of crack tip only. In addition, meshing is coarser around cracks that progressively stop. This effect is ascribed to the presence of a strain shielding zone, where mutual interactions are strong enough to stop any crack propagation. Figure-12 shows the evolution of the shielding zone associated with one given crack, as the later grows from 0.1mm up to 1mm. In figure-13, it is show that such calculations correctly estimates both mean and maximal crack depth up to 35,000 cycles.

CONCLUSION

Like in isothermal fatigue, a non-cracking regime has been identified in thermo-mechanical fatigue. This regime is associated with temperature variations smaller than 125 °C during SPLASH tests. This result is associated with particular conditions which include an initially planar surface ($Ra \leq 0.8$ µm) free of any

additional or residual stresses. In these conditions, with (Tmax = 550°C, $100 \leq \Delta T \leq 300$°C), crack initiation conditions on 316L steel can be deduced from isothermal low cycle fatigue data and methodology as reported in the RCC-MR code.

Crack growth of one isolated crack can be estimated thanks to a LEFM modelling, using a crack closure factor of q = 0.6. However, it must be emphasized that a value of q = 1.0 still gives a conservative prediction of crack growth rate.
The development of a thermal fatigue crack network presented two distinct stages. The first one refers to the initiation of a surface crack network. In the second stage, cracks extend in the depth direction only, while crack initiation completely stops. In this phase, a very important mutual crack shielding effect is evidenced. When considering this effect, crack growth predictions are in good agreement with observations, in spite of simplified assumptions. Maximum crack length can nevertheless be accurately determined for N < 35 000.

References

1. Gelineau, O., Sperandio, M., Martin, P., Ricard J.B., Martin, L., Bougault, A. (1994), Specialist's meeting on "correlation between material properties and thermohydraulics conditions in LMFRs"

2. F. de Keroulas, B. Thomeret, (1990) SFEN Volume 1 p. 107 – 117.

3. Code RCC – MR – Filière Neutron Rapide, Tome 1, Volume B, AFCEN (1985).

4. Starkley, M. S., Skelton, RP. (1982) Fatigue of Engineering Materials and Structures Vol.5 p. 329 – 341.

5. Haigh, J. R., Skelton, R.P. (1982) ASTM STP 770 p. 337 – 381.

6. Skelton, R. P. (1983) Fatigue at high temperature Applied Science Publications, p. 1 – 61

7. Skelton, R. P. (1990) High Temperature Technology Vol 8 n°2 p.75 – 88.

8. Dowling, N. E. (1977) ASTM STP 637 p. 97

9. Buchalet, C. B., Bamford, W. H. (1976) Mechanics of Crack growth, ASTM STP 590, p. 385 – 402.

10. Tavassoli, A. A. (1995) Fusion Engineering and Design Vol 29 p. 371 – 390.

11. Burlet, H., Vasseur, S., Besson, J., Pineau, A. (1989) Fatigue engineering Materials 12 – 2 p. 123

12. Fissolo, A., Marini, B. (1998) Proceeding of the ECF12 conference p. 31 – 36.

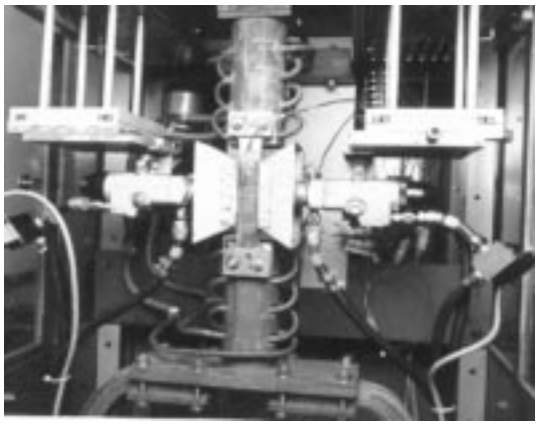

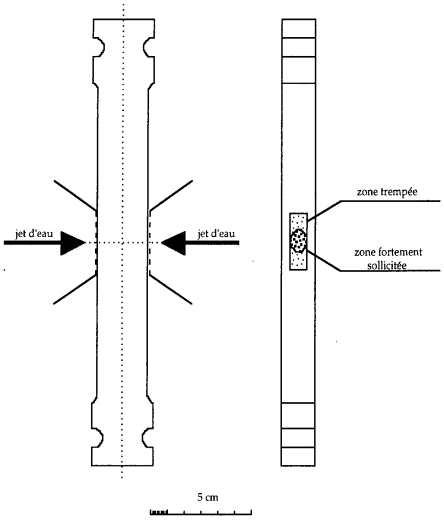

Facility

Specimen

Figure 1 : SPLASH thermal fatigue test.

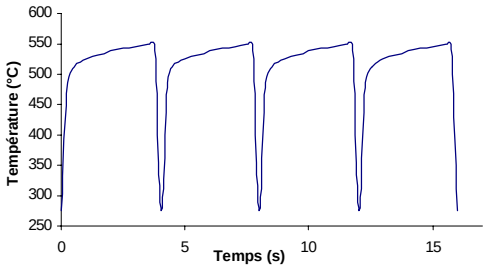

Figure 2 : Typical temperature variations at the surface of a SPLASH specimen, during one cycle.

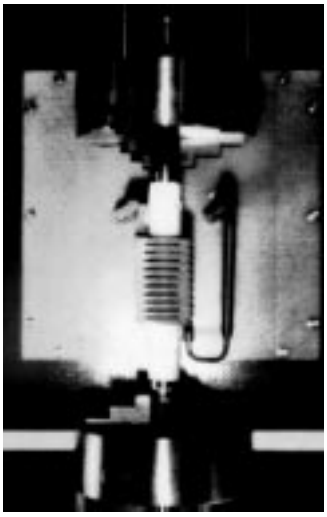

Figure 3 : CYTHIA thermal fatigue facility test.

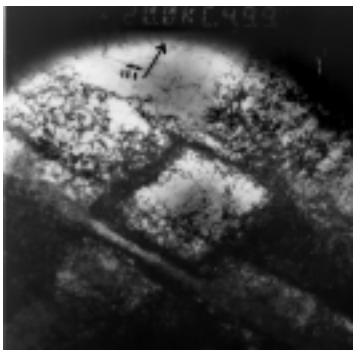

Figure 4 : TEM micrography. Surface grains from a CYTHIA specimen submitted to 100 cycles

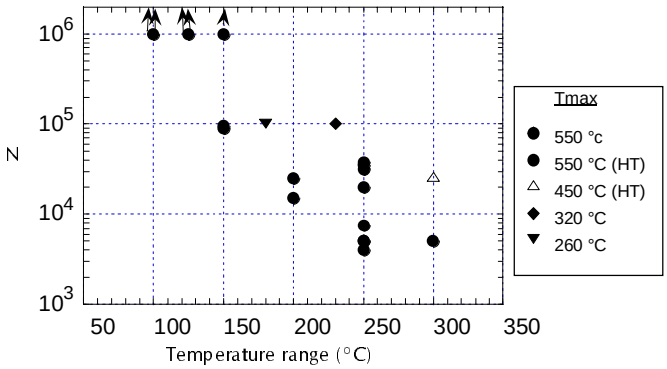

Figure 5 : Number of cycles to initiate cracking as a function of the temperature variation.

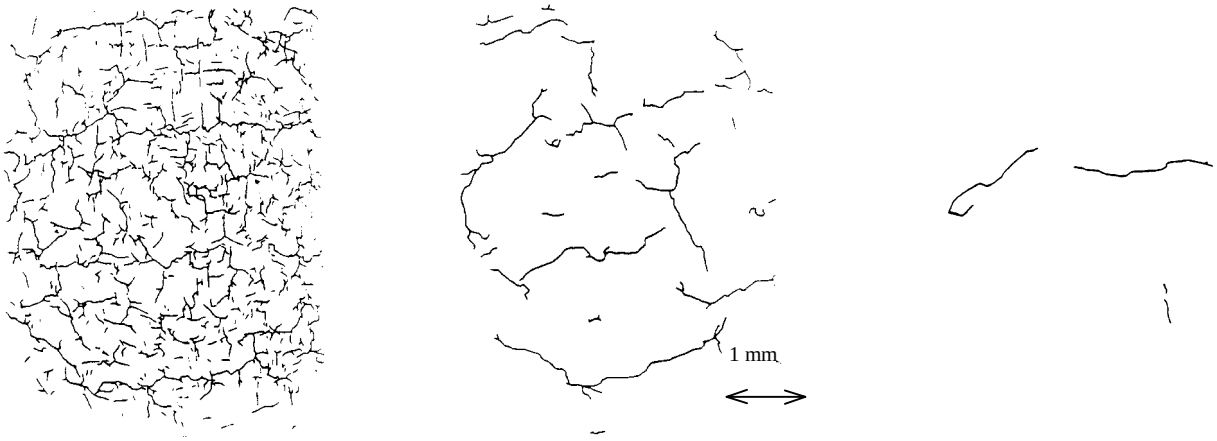

en surface 209 µm 569 µm

Figure 6 : Surface and sub-surface morphology of the cracking network after N = 20 000 cycles.

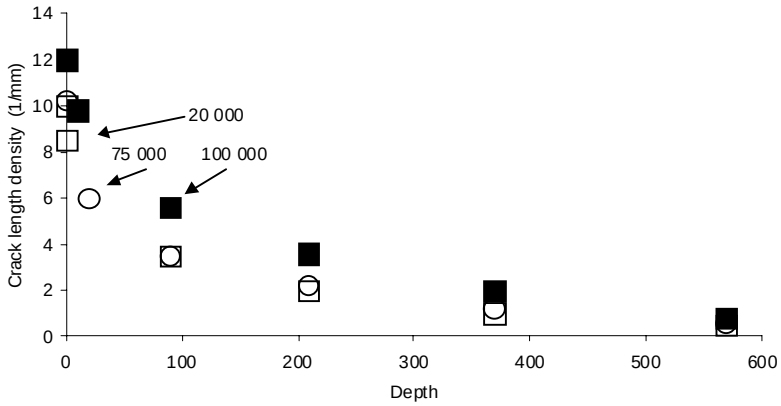

Figure 7 : Crack density as a function of depth. Examinations performed following the step by step removal of thin surface layers.

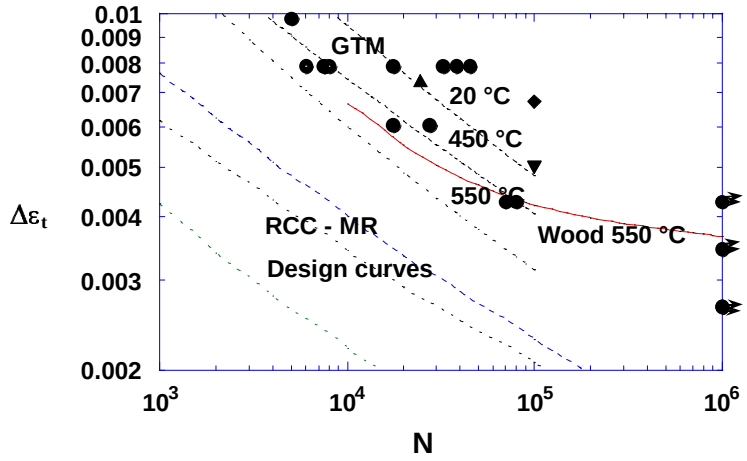

Figure 8 : Crack initiation tests. Comparison of the thermal fatigue results with the isothermal strain controlled fatigue curves.

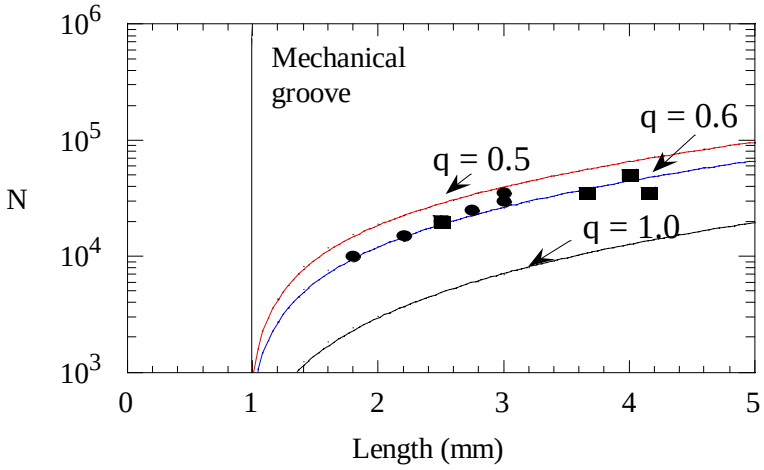

Figure 9 : Crack growth tests for a single, isolated crack. Crack depth as a function of number of cycles.

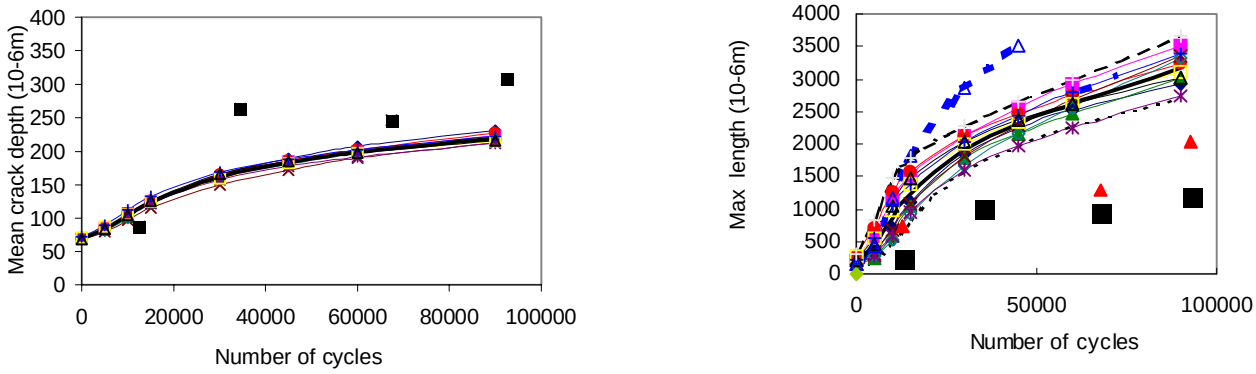

Figure 10 : Modelling of multiple crack growth using random surface initiation and accounting for the most influent crack-crack interactions only. Mean and maximum depths as a function of the number of cycles.

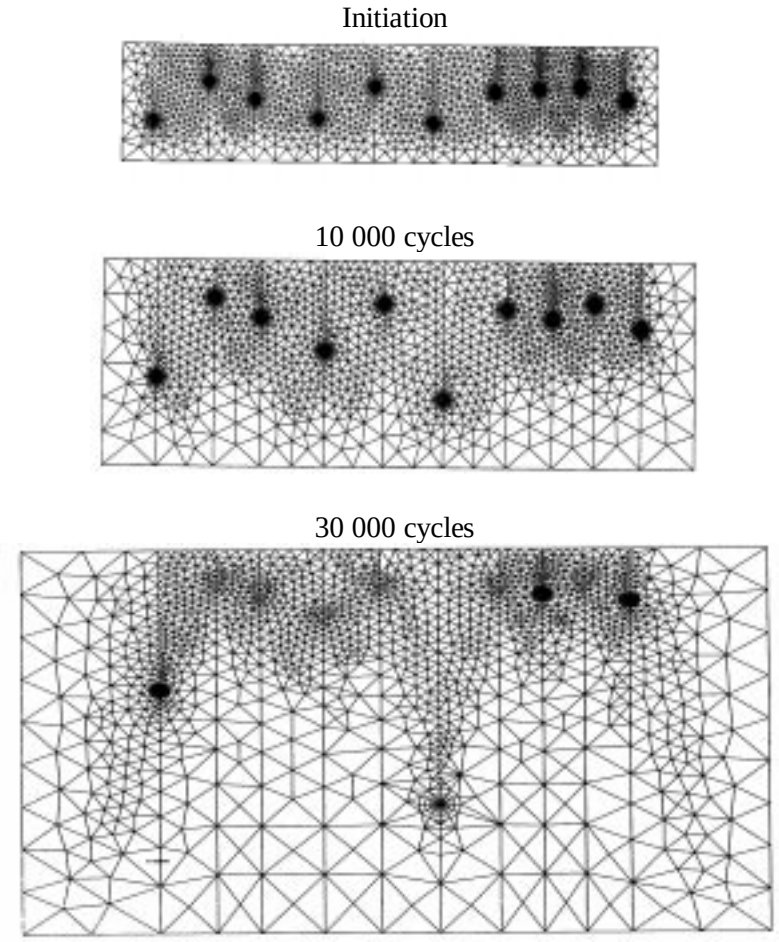

Figure 11 : Modeling of multiple crack growth using random initiation and accounting for the complete crack-crack interactions between 10 cracks, using auto-adaptative finite elements. Snapshots of the crack extension in the depth direction.

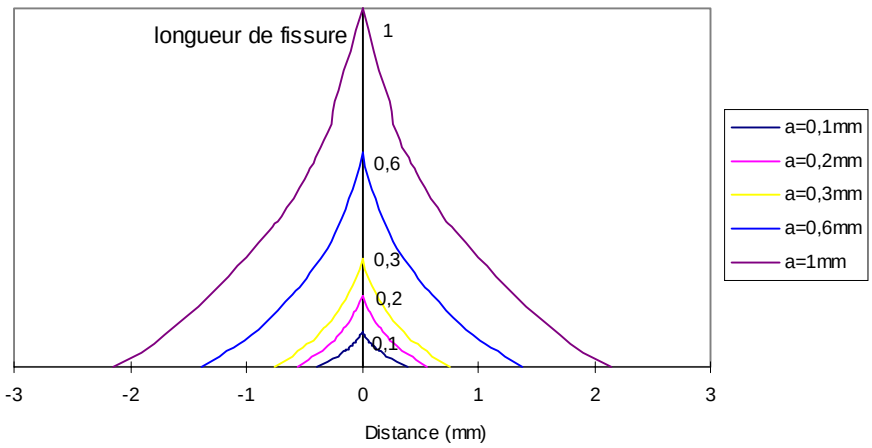

Figure 12 : Extension of the shielding zone associated with one crack, as it grows from 0.1mm up to 1mm.

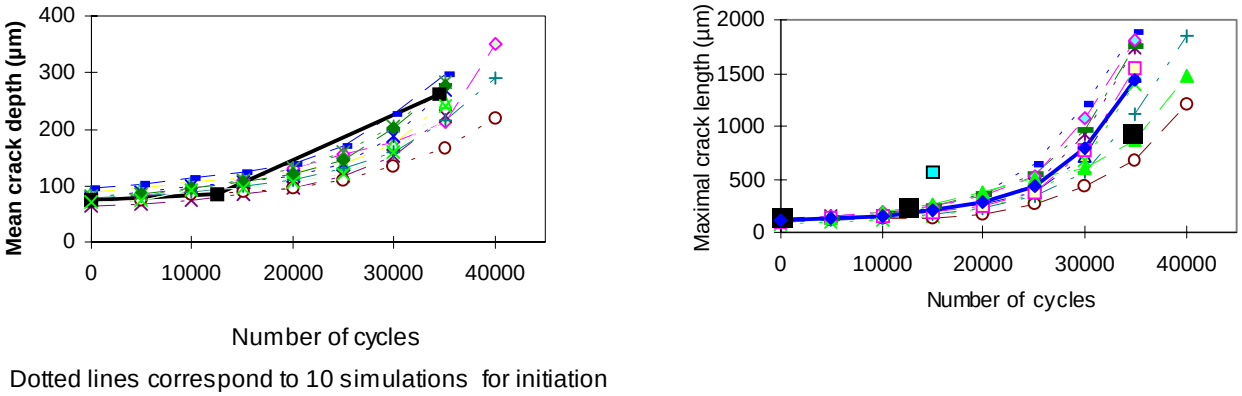

Figure 13 : Modelling of multiple crack growth using random initiation and accounting for the complete crack-crack interactions between 10 cracks. Mean and maximum depth as a function of number of cycles.